Association of a Protein with Membrane Vesicles at the Collisional Limit: Studies with Blood Coagulation Factor Va Light Chain Also Suggest Major Differences between Small and Large Unilamellar Vesicles†

Alan J. Abbott and Gary L. Nelsestuen*
Department of Biochemistry, The University of Minnesota, St. Paul, Minnesota 55108
Received March 3, 1987; Revised Manuscript Received July 17, 1987

ABSTRACT: Vesicle size can be a very sensitive modulator of protein–membrane association. In addition, reactions at the collisional limit may be characteristic of many types of protein–membrane or protein–receptor interactions. To probe these effects quantitatively, we analyzed the association of blood clotting factor Va light chain (Va-LC) with phospholipid vesicles of 15–150-nm radius. The number of protein binding sites per vesicle was approximately proportional to vesicle surface area. Association rates approached the collisional limit, and the activation energy for the association reaction was 4.5 ± 0.5 kcal/mol. In agreement with diffusional theory for this type of interaction at the collisional limit, the observed association rate constant for filling all sites was approximately proportional to the inverse of vesicle radius. This general property has important implications for many systems such as blood coagulation including possible slower association rates and higher K_m values for reactions involving whole cells relative to those obtained for phospholipid vesicles. Dissociation rate constants for reactions that are near the collisional limit should also be proportional to the inverse of vesicle size if diffusional parameters are the only factors influencing dissociation. However, Va-LC bound to small unilamellar vesicles (SUVs, ≤15-nm radius) gave slower dissociation rates than Va-LC bound to large unilamellar vesicles (LUVs, ≥35-nm radius). This indicated a change in K_I, the intrinsic protein–phospholipid affinity constant for LUVs vs SUVs. The cumulative effect of association and dissociation rates resulted in higher affinity of Va-LC for SUVs than LUVs under equilibrium conditions. The latter was corroborated by competition binding studies. Furthermore, the temperature dependence of both rate constants indicated an entirely entropy-driven binding to LUVs but a largely enthalpy-driven binding to SUVs. Interactions which are largely entropic are thought to be ionic in nature. The differences observed between binding to LUVs and SUVs may reflect thermodynamic differences between these types of phospholipid structures.

Membrane-bound enzymes and receptors constitute important types of interactions which are influenced by the general properties of membrane structure. Several steps of the blood coagulation cascade are localized on membrane surfaces [for a review, see Jackson and Nemerson (1980)]. For the prothrombinase complex, factor Va is a cofactor protein which associates with the membrane and binds the enzyme (factor Xa) and the substrate (prothrombin) (Nesheim et al., 1981; Lindhout et al., 1982; van de Waart et al., 1984). Due to high-affinity interactions, assembly events in blood coagulation constitute models for the general phenomenon of protein binding to membranes or membrane-bound receptors. Factor V also binds directly to the phospholipid molecules in the membrane and may be a sensitive probe for detecting changes in membrane phospholipid structure.

From the standpoint of protein-membrane interactions in general, special interest is related to association rate processes which may be limited by the rate of collision between the protein and the membrane–receptor particle (Berg & Purcell, 1977). In almost every protein–membrane system, association rate constants are well below the collisional rate constants for one protein and one membrane particle (Cuatrecasas, 1971; Frazier et al., 1974). However, unlike free protein receptors, membrane-associated receptors are clustered on a large particle so that many collisions are needed to fill the receptors. Individual rate constants then become a function of membrane particle concentration and the number of sites per particle (Delisi & Wiegel, 1981). Reactions at the collisional limit have been shown experimentally for protein–DNA interactions (Berg et al., 1981) and have been extended to membranes from a theoretical standpoint [e.g., see Berg (1985) and references cited therein]. Association rate constants for factor V–membrane binding, corrected for the number of proteins associated with each membrane particle, approximated the collisional rates between protein and vesicle (Pusey et al., 1982). Such a reaction may therefore constitute a model system for collisionally limited reactions at a membrane surface.

Although fundamental differences between large unilamellar vesicle (LUV)[1] and SUV structure are well-known, functional differences are not well understood. For example, the area per phospholipid is quite different (Gaber & Peticolas, 1977; Huang & Mason, 1978). Phospholipid packing structure affects internal motions of the phospholipid molecules (Sheetz & Chan, 1972), density of charge at the membrane surface (Mclaughlin, 1977; Chung et al., 1985), the water structure at the surface (Gruen et al., 1984; Melchior & Morowitz,

† Supported in part by Grant HL-15728 from the National Institutes of Health.

[1] Abbreviations: binding site refers to a single protein–membrane interaction; the term "site" is used for simplicity although it is understood that the site is not necessarily a discreet entity but consists of a combination of phospholipid molecules; Va-LC, approximately 80 000-dalton light chain of blood coagulation factor Va (Esmon, 1979); PC, phosphatidylcholine; PS, phosphatidylserine; dansyl-PE, *N*-dansyldipalmitoylphosphatidylethanolamine; EDTA, ethylenediaminetetraacetic acid; LUV, large unilamellar vesicle (≥35-nm radius); SUV, small unilamellar vesicle (≤15-nm radius); Tris, tris(hydroxymethyl)aminomethane; SDS, sodium dodecyl sulfate.

0006-2960/87/0426-7994$01.50/0

1972), and the degree of phospholipid hydrocarbon exposure to the aqueous environment. Binding preference for LUVs or SUVs could arise from several types of protein–membrane interactions (i.e., H-bonding, electrostatic, or hydrophobic interactions) potentially affected by these structural differences. For example, the tetravalent cation gentamycin binds to LUVs with 10^3 times its affinity for SUVs (Chung et al., 1985). Proteins such as cytochrome b_5 (Greenhut et al., 1986) and complement proteins (Silversmith & Nelsestuen, 1986), which appear to insert into the hydrocarbon portion of the membrane, have been found to preferentially associate with SUVs.

For factor V and its membrane binding peptide, Va-LC, equilibrium binding studies have provided a range of affinity constants that leave important questions unresolved. Both normal and activated platelets bind Va tightly ($K_d \approx 10^{-10}$–10^{-11} M; Tracy et al., 1979, 1981). While similar affinities have been reported for factor Va binding to small phospholipid vesicles (SUVs) containing 20–40% negatively charged phospholipids (Pusey et al., 1982), simple correlation of affinity constants does not establish the similarity of binding mechanisms (Pusey & Nelsestuen, 1984). A separate study, using alternative methodology, found that factor V binding to LUVs showed an affinity of about 10^{-8} M (van de Waart et al., 1983). While factor Va bound to phospholipid monolayers spread at different surface areas per phospholipid, the actual binding constants were found to be less than nanomolar (Mayer et al., 1983), and large fluctuations could occur below this value. Large changes in phospholipid packing are associated with phase transitions (Wiegel, 1984), and factor V–membrane binding stoichiometry dropped dramatically for dimyristoylphosphatidylcholine–dimyristoylphosphatidylserine vesicles below the phase transition. A concomitant change in K_d has not been demonstrated (van de Waart et al., 1987). While factor Va–membrane binding showed high sensitivity to salt, other extrinsic membrane proteins which share its affinity for negatively charged phospholipid surfaces [e.g., myelin basic protein (Boggs & Moscarello, 1978a) and apocytochrome *c* (Gorrisen et al., 1986)] display properties of both electrostatic and nonelectrostatic binding. This distinction has been addressed by labeling Va-LC bound to SUVs with the lipophilic, photoactivated probe 3-(trifluoromethyl)-3-(*m*-[^{125}I]iodophenyl)diazirine (Krieg et al., 1987). Since lipophilic probes label bound and free protein to only slightly different degrees, the extent of lipophilic interaction by Va-LC is not clear (Mayer, 1983).

This study examined the binding of Va-LC to phospholipid membranes. Association rates were consistent with a collisionally limited binding mechanism so that the experimentally obtained association rate constant was dependent on vesicle size and on the number of sites per vesicle. Dissociation rate constants and equilibrium competition data indicated that SUVs bind Va-LC more tightly than LUVs. The binding of Va-LC to SUVs was fundamentally different from its binding to LUVs; the net free energy of factor Va-LC binding was largely enthalpic for SUVs, while it was almost entirely entropic for LUVs. This difference may reflect the types of internal forces that distinguish LUVs and SUVs.

Materials and Methods

Phosphatidylcholine (PC) from egg yolk, PS from bovine brain, and dansyl-PE were purchased from Sigma Chemical Co. The reported purity was >98%, and the phospholipids were used without further purification. All buffers contained 0.05 M Tris at pH 7.5 plus the indicated concentrations of NaCl, $CaCl_2$, and EDTA.

Bovine factor V was isolated from bovine blood by the method of Pusey et al. (1982). Va-LC was prepared as described by Lindhout et al. (1982) after activation of factor V by thrombin (1:1000 w/w). Gel electrophoresis of purified Va-LC in the presence of SDS (Laemmli, 1970) showed a major band of M_r 80 000 and two minor components of M_r 50 000 and M_r 30 000. The latter were presumed to be degradation products of the M_r 80 000 band. Similar degradation products generated by the action of protein C on factor Va showed no change in membrane binding properties (van de Waart et al., 1984). The studies reported here were conducted without further purification. The weight concentrations of membrane binding protein in the Va-LC preparations were estimated from light-scattering changes observed when Va-LC was mixed with small phospholipid vesicles. The mass of membrane-bound protein was calculated by the method of Nelsestuen and Lim (1977). The molar concentration of Va-LC was estimated by using a molecular weight of 80 000 (Lindhout et al., 1982).

Vesicle Preparation. Small unilamellar vesicles (SUVs) were generated by sonication and subsequent gel filtration as described previously (Nelsestuen & Lim, 1977). Large vesicles were prepared by ether injection and extrusion techniques. Ten milligrams of phospholipid dissolved in 2–3 mL of anhydrous ether was injected slowly into 4–6 mL of buffer maintained at 60 °C (Deamer & Bangham, 1976). These vesicles were extruded through a 0.6-μm polycarbonate filter to break up large aggregates, and the product was gel filtered on Sephadex S-1000. The largest vesicles, eluting at the void volume, were passed through successively smaller pore filters (Nucleopore Corp., Pleasanton, CA) of 0.4, 0.1, and 0.05 μm to obtain vesicles of the desired size (Hope et al., 1985). The hydrodynamic radii of the vesicle populations were determined by quasi-elastic light scattering (Bloomfield & Lim, 1978) using a Langely Ford Model LSA2 spectrophotometer coupled to a (Model 1096) correlator. Diffusion constants were converted to radii of hydration for spherical diffusing particles by the Stokes–Einstein equation. The *Z*-averaged particle radii are reported here. The average particle distribution of vesicles has been documented for extrusion (Mayer et al., 1986) and sonication (Nelsestuen & Lim, 1977) vesicles. For observation of general properties as shown here, corrections for size distribution were not carried out.

Fluorescence Measurements. Va-LC–membrane binding was monitored by fluorescence energy transfer from tryptophan residues in the protein to dansyl-PE in the vesicle. Fluorescence was monitored with an SLM Instruments Model 4800 fluorometer. Excitation light (280 nm) was from a xenon arc lamp with a 16-nm slit width. Dansyl fluorescence was monitored by using a 500-nm cutoff emission filter (Corion Corp.).

Quantitation of Binding Sites. Phospholipid vesicle solutions (0.5 μg of phospholipid) were titrated with Va-LC under low-salt (0.025 M NaCl) conditions. The concentration of binding sites was estimated by extrapolating the initial linear portion of the binding curve to the level of saturation (see below). The number of binding sites per vesicle of 15-nm radius has been estimated to be about 75 (van de Waart et al., 1983; Higgins & Mann, 1983; Pusey & Nelsestuen, 1984). The number of sites on other vesicle sizes was assumed to be directly proportional to vesicle surface area (100-fold range for the vesicles used). The validity of the latter assumption was indicated by the total binding capacity per unit weight of phospholipid which was within about 25% of that anticipated for the different vesicles (see below).

Association Rate Measurements. Va-LC (5.7 nM), sufficient to provide a 4-fold excess of protein over protein binding sites on the vesicles, was added to 0.1 μg of labeled vesicles (PS/PC/dansyl-PE, 20:75:5) in 1.5 mL of buffer (0.05 M Tris, 0.025 M NaCl, and 50 μM EDTA, pH 7.5). The solution was continually stirred. Under these conditions (low salt, 10 °C), the dissociation rate was negligible on the time scale of the association process (Pusey et al., 1982). This pseudo-first-order reaction was analyzed by the integrated rate expression:

$$\ln (B_t/B_0) = k_{app}[\text{Va-LC}]_0 t$$

where k_{app} is the second-order rate constant for association and B_t/B_0 is the ratio of the concentrations of free to total binding sites at time t. Since the fluorescence signal (F_t) is proportional to filled binding sites, $B_t/B_0 = (F_\infty - F_t)/F_\infty$. Plots of $\ln (F_\infty - F_t)/F_\infty$ vs time were linear for at least 50% of the reaction (see below). For studies dependent primarily on comparison values, rate constants were derived from reaction half-times ($t_{0.5}$) where $t_{0.5} = 0.693/k_{app}[\text{Va-LC}]_0$. To confirm that conditions were pseudo first order, association rate constants for 150-nm radius vesicles were measured with 5.7, 11.4, and 17.1 nM V_a-LC. The reaction half-times descreased in the manner anticipated for a pseudo-first-order reaction (23, 12, and 8 s, respectively) to give a constant k_{app} for the reaction. A 3-fold decrease in the phospholipid concentration had no effect on the association half-life. All association reactions were performed in triplicate, and the averaged values are reported. However, reproducibility was high and with less than 10% variation between replicate samples run in sequence. Standard deviations for replicate determinations were small and are not shown.

Dissociation Rate Measurements. The method of Pusey et al. (1982) was used. Briefly, the fluorescence due to tryptophan to dansyl-PE energy transfer in a Va-LC–membrane complex was determined. At zero time, a large excess of unlabeled SUVs [20 μg of PC/PS (60:40) in 0.1 mL of buffer] was injected quickly (dead time of 1 s) into 1.5 mL of solution containing 1 μg of labeled vesicles plus bound Va-LC. Va-LC dissociation from the fluorescent vesicles was measured as a decrease from the initial fluorescence. For routine comparisons, dissociation rates (k_{dissn}) were from the first reaction half-time, $t_{0.5} = 0.693/k_{dissn}$. While several properties appeared to influence dissociation rates, the important parameters were derived from *relative* changes in the k_{dissn}, and these relative changes were similar for rate constants obtained from any level of dissociation (e.g., 25%, 50%, or 75% of dissociation reaction). Dissociation rate studies were performed in triplicate, and the averaged values are shown. However, replicates were virtually indistinguishable (<10% variation), and standard deviations were not calculated.

Equilibrium Competition Experiments. One microgram of SUVs containing dansyl-PE was mixed with various amounts of competing unlabeled vesicles in 1.5 mL of buffer. An amount of Va-LC, adequate to reach 30% saturation of the fluorescent vesicles, was added, and fluorescence intensity due to energy transfer was measured. The measured fluorescence (F) divided by that obtained in the absence of competing vesicles (F_0) provided an estimation of the fraction of Va-LC bound to the fluorescent vesicle population. All fluorescence measurements shown are due to energy transfer, and backgrounds from the components or from direct excitation of the dansyl-PE have been subtracted.

RESULTS

Quantitation of Binding Sites. Fluorescent phospholipid vesicles of identical composition and three sizes were generated as indicated under Materials and Methods, and their properties are shown in Table I. Titration of each preparation with Va-LC gave linear curves suggesting quantitative protein–membrane binding for at least the first 50% of the reaction. A 10-fold increase in phospholipid concentration gave a similar initial slope (not shown). This property was in agreement with previous work (Pusey et al., 1982) that reported binding affinities for SUVs of $K_d < 5$ nM. This limit appeared to apply to all vesicles used in this study.

Table I: Physical Properties of Phospholipid Vesicles

vesicle preparation method	D (cm²/s) × 10⁸ [a]	R_h (μm) [b]
sonication and gel filtration	10.9 ± 0.003	0.0155 ± 0.003
extrusion (0.4-μm membrane)	1.06 ± 0.1	0.150 ± 0.015
extrusion (0.1-μm membrane)	3.14 ● 0.1	0.050 ± 0.003
extrusion (0.05-μm membrane)	4.64 ± 0.1	0.035 ± 0.003

[a] D is the translational diffusion constant measured by quasi-elastic light scattering; see Materials and Methods. [b] This is the hydrodynamic radius calculated from D by using the Stokes–Einstein equation.

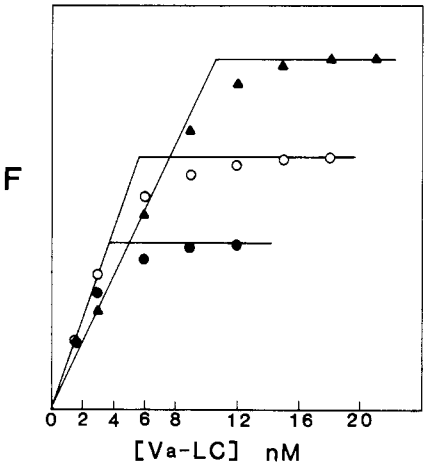

FIGURE 1: Titration of phospholipid vesicles with Va-LC. Phospholipid (0.5 μg of PC/PS/dansyl-PE, 75:20:5) in 1.5 mL of buffer (0.05 M Tris, 0.025 M NaCl, and 50 μM EDTA, pH 7.5) was titrated by addition of Va-LC. The increase in fluorescence represents binding to vesicles of 15- (▲), 37.5- (○), and 150-nm (●) radius. Va-LC concentrations represent total added protein.

The linear portion of the curve was extrapolated to the saturation point to obtain the total number of binding sites in the solution (Figure 1, solid lines). The number of binding interactions per unit weight of phospholipid varied somewhat for the different vesicle preparations (Figure 1). This was expected for two reasons. First of all, SUVs with 15-nm outer radius should have 33% more sites than large vesicles. Since the inner radius of SUVs is only about 11 nm, the inner to outer surface area ratio is 1:2 whereas for LUVs this ratio is 1. Therefore, 66% of the total phospholipid is in the outer monolayer of SUVs, and approximately 50% of the phospholipid is in the outer monolayer of LUVs. Second, small amounts of multilamellar membranes in the LUVs (Hope et al., 1985) would decrease the concentration of accessible phospholipid. Furthermore, variation in the amount of multilamellar character in different LUV preparations may be the primary basis for the maximum of 25% variation in the maximum capacity of various LUV preparations used in this study. The Va-LC binding capacity of SUVs was virtually the same for all preparations. Thus, it was essential to determine the actual binding capacity per mass of lipid for each LUV preparation.

Although binding in Figure 1 was too tight to allow quantitative estimation of the binding constants, some qualitative characteristics were apparent. Binding appeared to be linear

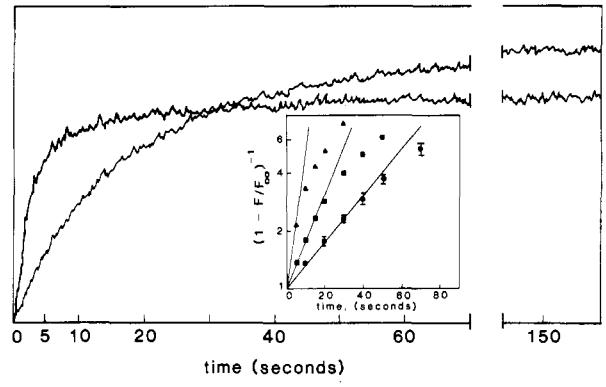

FIGURE 2: Association kinetics of Va-LC with phospholipid vesicles of different sizes. Va-LC (5.7 nM) was mixed with 0.1 μg of labeled vesicles (adequate to give 1 nM binding sites), and the fluorescence change was recorded. The faster and slower tracings were obtained for 15-nm and 150-nm radius vesicles, respectively. Inset: The association rate data were replotted in the logarithmic form expected for a pseudo-first-order association for the 15- (▲), 37.5- (■), and 150-nm (●) radius vesicles. Other conditions were given in Figure 1.

up to 75% saturation of 15-nm vesicles but to only 50% saturation with LUVs. This qualitative property suggested that Va-LC bound to SUVs with higher affinity than to LUVs. Another property was a lower fluorescence energy transfer per Va-LC molecule bound to SUVs (about 80% of that for LUVs). Although small, this difference was consistently observed and suggested a slightly different relationship between protein tryptophans and membrane dansyl groups for Va-LC bound to LUVs vs SUVs. A number of factors could produce this difference including the fact that the curved surface geometry of SUVs would increase the distance between protein tryptophans and dansyl-PE located near the protein. The basis for this small difference in energy transfer was not pursued.

Association Rates. Earlier studies indicated that Va-LC binds to SUVs at approximately the theoretical collisional rate (Pusey & Nelsestuen, 1984). This property can be further tested by comparing the effects of membrane particle size. The theoretical rate constant for collision between spherical particles (k_{coll}) can be obtained from Smoluchowski's theory (1917):

$$k_{coll} = 4\pi N_{av} DR/1000 \quad (1)$$

where D is the sum of the vesicle and protein diffusion constants (essentially equal to that of the smaller protein particle in this case) and R is the sum of their radii (approximately equal to that of the vesicle). However, with N binding sites per vesicle, the experimentally observed rate constant (k_{app}) for filling the sites at the collisional limit becomes

$$k_{app} = k_{coll}/N \quad (2)$$

In cases where N is related to the total surface area of the membrane particle, each binding site has a constant area (A), $N = 4\pi R^2/A$. Combination of these relationships shows the relationship between particle size and k_{app} for a reaction functioning at the collisional limit:

$$k_{app} = (DN_{av}/1000)A/R \quad (3)$$

A plot of k_{app} vs $1/R$ should give a slope proportional to A.

This predicted behavior was tested for Va-LC. Identical concentrations of Va-LC were mixed with phospholipid vesicles of different radii but with identical numbers of total protein binding sites in solution (Figure 2). Under pseudo-first-order conditions (excess protein), the results showed substantially different rates for the different vesicles (Figure 2). As seen in Figure 2 (inset), the logarithmic relationship for a pseudo-first-order reaction was approximately obeyed for 60–75% of the reaction. The curvature near saturation could result from several factors such as reduction in available sites (N, see below) and resulting loss of collisional efficiency (see below). Alternatively, limited polydispersity of the vesicle preparations should result in curved plots; since k_{app} is proportional to R, the smaller vesicles will fill faster, and curvature will occur as the last sites on the larger vesicles are filled. The actual basis for limited curvature near saturation was not determined, and, for purposes of comparison studies, k_{app} was estimated from the first reaction half-time. The pseudo-first-order nature of these reactions was demonstrated by an inverse linear relationship between reaction half-time and protein concentration (see Materials and Methods).

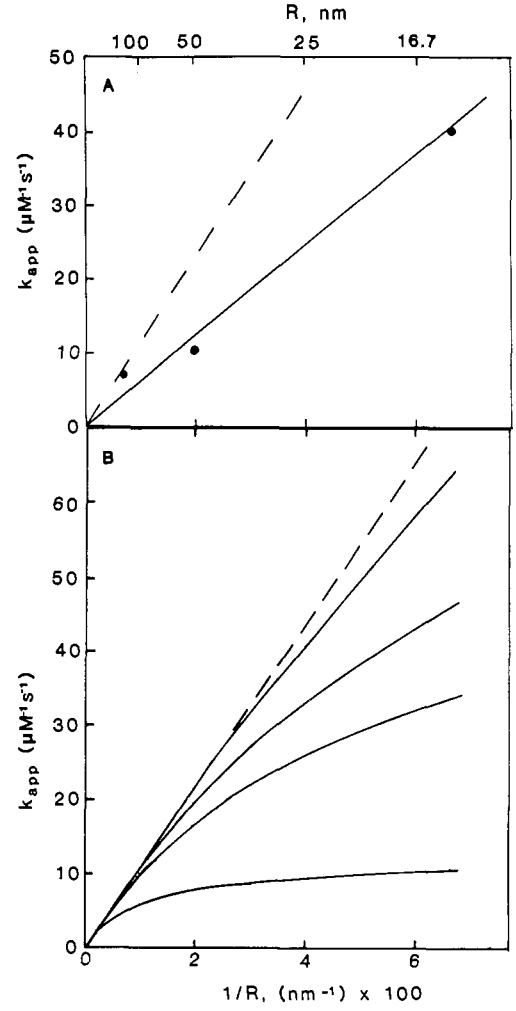

FIGURE 3: Dependence of k_{app} on vesicle radius (R_v). Panel A shows the relationship between k_{app} (●), calculated from the half-time (see Materials and Methods) of the association reactions (obtained as in Figure 2) and compared to the theoretical maximum rate constant (dashed line) calculated from diffusion constants, Stokes radii, and number of sites per vesicle [see eq 2 and Pusey et al. (1982)]. Panel B shows the theoretical deviation from the collisional limit (dashed line) for the interaction of a protein with sites on a membrane particle. The sites are of uniform density (calculated from 75 binding sites per particle of 15-nm radius) but of decreasing radii (s, eq 4): 3.46 nm for the uppermost curve, 1 and 0.5 nm for the intermediate curves, and 0.1 nm for the lowermost curve.

A plot of k_{app} vs $1/R$ agreed qualitatively with the behavior anticipated for a collisionally limited reaction of this type (Figure 3A). The value for A obtained from the line drawn in Figure 3 was 19.4 nm^2. The binding site area calculated from protein to membrane mass at saturation was 37 nm^2. This difference reflects the difference between theoretical and

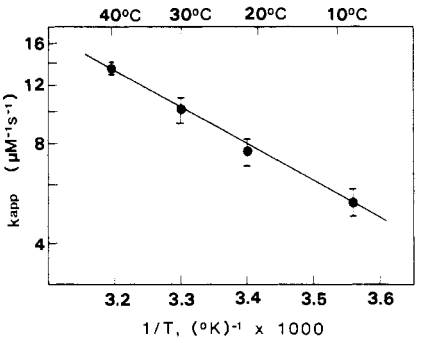

FIGURE 4: Temperature dependence of Va-LC association for LUVs. Measurement of k_{app} was as described in Figure 2 for 150-nm radius vesicles at temperatures between 40 and 10 °C. Other conditions were given in Figure 1. The E_a obtained from the line drawn was 4.5 kcal/mol.

observed rate constants (Figure 3A).

The estimated association rate constants obtained were 50–90% of the calculated collisional rate constants (see Figure 3A). A real deviation from the theoretical value could result if Va-LC existed in membrane binding and nonbinding conformations. In this case, the theoretical association rate would be lowered by the fraction of protein in the nonbinding state at any one time. Such a property would not change the *relative* behavior predicted by eq 3. However, limitations in theoretical calculations and experimental measurements did not allow determination of whether or not the observed difference was significant. For example, the proteins are not spherical, and hydrodynamic radii were used in eq 1. Furthermore, the radii of the vesicles were *Z*-averaged values which will emphasize the larger particles in a somewhat disperse preparation. Mayer et al. (1986) compared the *Z*-averaged diameter of vesicles prepared by similar extrusion methods and the number-averaged diameter. Number- and *Z*-averaged radii should represent high and low estimates of the actual diameter (Cantor & Schimmel, 1980). The different measurements demonstrated an 8% difference for vesicles of 74-nm diameter (*Z*-averaged value). Thus, within the probable limitations of this study, the properties of this protein–membrane interaction agreed with a collisionally limited reaction with a similar area per membrane-bound protein for all vesicles.

The temperature dependence of k_{app} for vesicles of 150-nm radius was examined and is shown in Figure 4. The Arrhenius activation energy was 4.5 ± 0.5 kcal/mol. Rapid-mixing techniques are needed to obtain rates for SUVs at elevated temperatures. Previous studies gave an activation enthalpy for vesicles for 15-nm radius of 6.5 kcal/mol which was also close to the value for a diffusionally controlled reaction (Pusey, 1982). Thus, association of factor Va with SUVs and LUVs appeared to be a diffusionally controlled reaction throughout the temperature range examined.

Theoretically, a limiting value for k_{app} exists and is illustrated in Figure 3B by the approach to a horizontal plot. This limit for k_{app} will coincide with the value for association of protein with individual receptors that are free in solution. This limitation is apparent from eq 4 which consists of eq 2 modified

$$k_{app} = (k_{coll}/N)[Ns/(Ns + \pi R)] \quad (4)$$

by a probability factor $[Ns/(Ns + \pi R)]$ that corrects for inefficient searching at the particle surface. The latter is a feature of all association rate constants (Berg & Purcell, 1977). In this equation, s is the radius of an actual binding site on the membrane surface, and R is the radius of the membrane particle. That approach to a horizontal limit for the plot in Figure 3B is inevitable can be shown by decreasing N until it approaches 1 (when N depends on surface area, decreasing R will also decrease N). At this point, the lone remaining site is independent of all other sites, the denominator in eq 4 is dominated by πR, and this R term is cancelled by the R term in k_{coll} (eq 1). Normally, the horizontal limit should be reached long before $N = 1$. Alternatively, approach to the horizontal limit will result from smaller s (as illustrated in Figure 3B) which is analogous to a more restricted binding interaction; as s decreases, each binding event requires a more thorough search of the surface by the protein. Surface searching results from secondary collisions that occur between protein and membrane during a diffusional encounter complex. The duration of a diffusional encounter complex consists of the time between the collision of two particles (via eq 1) and diffusional escape and is approximately equal to R^2/D (Berg et al., 1981). The number of secondary collisions per encounter complex is proportional to R (Berg & Purcell, 1977) so that large membrane particles will experience more surface area searching than will small particles. The number of collisional events needed per binding event can require formation of many encounter complexes (that is, the probability of binding during any individual encounter complex is low). At this point, the reaction is far from the collisional limit, and k_{app} is independent of R.

An important ramification of these behaviors is that kinetic properties of systems located on small particles (such as vesicles) may be characteristic of the reactions below the collisional limit. The same systems located on large particles (such as cells) could be characteristic of the reactions at the collisional limit.

Dissociation Rates. The dissociation reaction can also show diffusion-related properties predicted from particle size and number of binding sites per particle. Dissociation is the result of two steps, a diffusional dissociation constant, k_2, and a unitless intrinsic equilibrium constant, K_I, or protein binding site affinity (Delisi, 1983):

$$\text{Pr} \underset{k_2}{\overset{k_1}{\rightleftharpoons}} \text{Pr*receptor} \underset{k_-}{\overset{k_+}{\rightleftharpoons}} \text{Pr–receptor} \quad (5)$$

$$k_{dissn} = k_2(k_-/k_+) = k_2K_I \qquad k_{assn} = k_1 \qquad K_I = k_-/k_+$$

where Pr is the protein, Pr*receptor is an arrangement that requires no further diffusion for binding, Pr–receptor is the protein bound to the vesicle, k_{dissn} is the overall experimentally observed dissociation rate constant, and k_{assn} is the experimentally determined association rate constant (k_{app} from eq 2 and 3). Once a protein has been released from its receptor, it is engaged in a diffusional encounter complex, and the number of recollisions of the protein with the membrane before escape to bulk solution is proportional to R (Berg & Purcell, 1977). Since reassociation could occur during any recollision, these diffusional parameters provide that the rate constant for the escape (k_{dissn}) should be approximately proportional to $1/R$. This property will only apply to reactions that associate at nearly the collisional limit.

First-order rate plots of dissociation were curved (Figure 5, inset) which was reported previously (Pusey & Nelsestuen, 1984). Negative cooperativity was lessened when initial binding was below 30% saturation of the initial membranes (data not shown). This behavior is predicted for collisionally limited reactions since the probability (P) of reassociation during a recollision is influenced by the proportion of free binding sites [$P = Ns/(Ns + \pi R)$; see eq 4 as well as Berg and Purcell (1977)]. Figure 6 shows theoretical plots of the effects of this property on the observed dissociation rate constant for reactions proceeding from 30% to 0% (upper

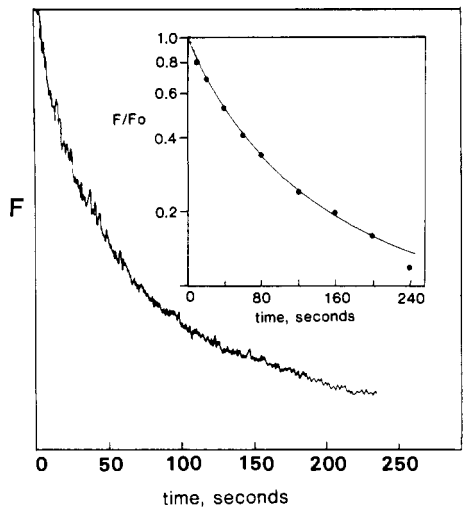

FIGURE 5: Dissociation of Va-LC from phospholipid vesicles. At zero time, unlabeled vesicles (20 μg of PC/PS, 60:40) were added to 1 μg of fluorescent-labeled vesicles (PC/PS/dansyl-PE, 75:20:5) that were 30% saturated with respect to Va-LC. Loss of fluorescence energy transfer from protein tryptophan to dansyl-PE due to dissociation of Va-LC was recorded with time. Inset: First-order plot of the data. The buffer (0.05 M Tris, 0.025 M NaCl, and 2 mM Ca^{2+}, pH 7.5) was chosen to give an easily measured dissociation rate. Qualitatively similar results were obtained in the absence of calcium.

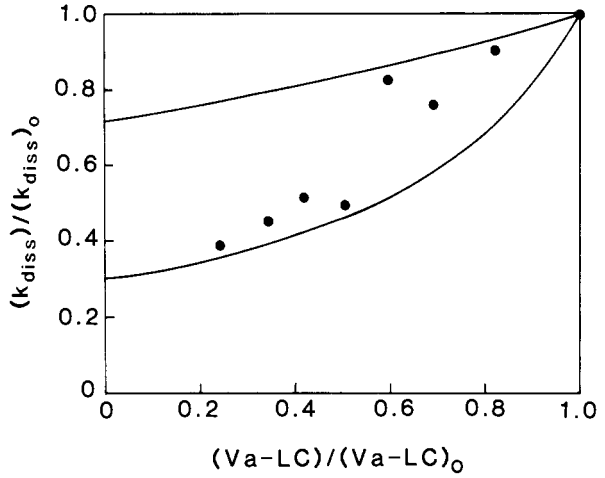

FIGURE 6: Changes in k_{dissn} with density of protein bound to the membrane. Theoretical curves for the anticipated decrease in k_{dissn} vs amount of bound protein were generated as described in the text. Initial conditions ($[Va-LC]/[Va-LC]_0 = 1$) were 30% saturation of all sites (upper curve) and 75% saturation of all sites (lower curve). Actual values for k_{dissn} (●) were obtained from the slope of a line drawn tangential to the first-order dissociation curve (e.g., Figure 5 inset). The experimental conditions used for these values included 150-nm radius LUVs that were initially 30% saturated (30% of maximum fluorescence intensity, Figure 1) with Va-LC. The other conditions are given in Figure 5.

curve) and from 75% to 0% (lower curve) of sites filled. In each case, the initial rate constant (i.e., at 30% or 75% filled sites) was normalized to 1.0. Curvature is more pronounced for dissociations beginning at a higher level of saturation. Also shown in Figure 6 are the experimental values for k_{dissn} measured from the actual dissociation curve (Figure 5, inset) with an initial saturation level of 30%. Linear tangents to these plots were obtained from the first-order dissociation curve. These were normalized to 1.0 for the rate constant at the outset of the dissociation reaction. The experimental values showed a greater curvature than predicted by reassociation probability alone (Figure 6). Consequently, it appeared that intrinsic binding constants, k_+ and k_- (eq 5), also changed with the degree of membrane saturation. This apparent negative co-

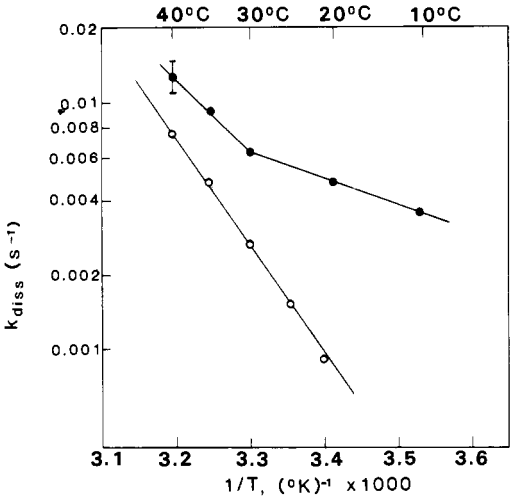

FIGURE 7: Temperature dependence of Va-LC dissociation. Dissociation rates obtained from the half-times for dissociation were recorded under the conditions given in Figure 5. Values obtained for SUVs [15-nm radius (○)] and LUVs [37.5-nm radius (●)] are shown. The standard deviation of replicate determinations was small except for the value presented with error bars shown.

operativity is anticipated for protein binding to multiple receptors (Dwyer & Bloomfield, 1981).

An unexpected finding was that dissociation was more rapid from LUVs than from SUVs. Since this was contrary to the behavior anticipated from diffusion factors alone (given above), it appeared that K_1 must be altered for the different vesicle populations. The temperature dependence of dissociation rates was determined for three different preparations of each vesicle size. The results were consistant, and Figure 7 shows the results of a typical experiment for vesicles of two sizes. The Arrhenius activation energy for dissociation from SUVs was 20 kcal/mol. This was about 4 times larger than the activation energy of association, indicating that the overall enthalpy for the binding at equilibrium, ΔH, was about −16 kcal/mol. This enthalpy change was comparable to the total free energy change associated with a binding interaction with a K_d of 10^{-11} M (ΔG = −15.1 kcal/mol).

The temperature dependence of dissociation from vesicles of 75-nm radius was quite different. Between 10 and 30 °C, the activation energy (4 ± 1 kcal/mol) was approximately the same or less than that for the association rate. Consequently, the overall enthalpy of binding to large vesicles was nearly zero. Entirely entropic binding interactions have been demonstrated for a number of associations between proteins and between protein and DNA. Only one other group of membrane binding proteins (vitamin K dependent proteins) has been found to display this behavior (Resnick & Nelsestuen, 1980).

At high temperatures, Va-LC–vesicle dissociation rates showed significant upward curvature of the Arrhenius plot such as that shown in Figure 7. While most preparations of LUVs displayed this curvature, it was often less than that shown here. The basis of this curvature was not investigated further but may be related to the basis of similar temperature-dependent behavior observed for several integral membrane protein activities in cellular systems [see Sackmann (1984) and references cited therein; Illsley et al., 1987; Worman et al., 1986; Livingstone & Schachter, 1980].

The general properties of temperature dependence for vesicles of 150-nm radius (data not shown) were similar to those of 37.5-nm radius. In fact, the only vesicles which showed the behavior of SUVs were of about 15-nm radius. The cutoff for SUV vs LUV behavior therefore seemed to be at a relatively small size.

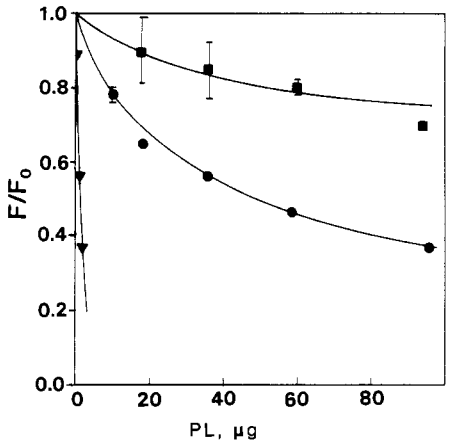

FIGURE 8: Comparative binding of Va-LC to SUVs vs LUVs. Mixtures of labeled SUVs (1 μg of PC/PS/dansyl-PE, 75:20:5) and the indicated amount of unlabeled (PC/PS, 80:20) LUVs [at 40 (●) and 10 °C (■)] or SUVs [at 40 and 10 °C (▲)] were prepared. A limiting amount of Va-LC (1 nM) was added, and the amount bound to the labeled vesicles as a fraction of the total was measured. F_0 is the fluorescence obtained with no unlabeled vesicles, and F is the fluorescence obtained in the presence of the amount of unlabeled vesicles indicated. Other conditions are given in Figure 5.

The combined observations in Figures 1 and 7 indicated that Va-LC bound to SUVs and LUVs in fundamentally different manners and with different affinities. Competition binding studies were carried out to corroborate these findings. Va-LC bound to fluorescent-labeled SUVs was removed by addition of competing, unlabeled vesicles of different sizes (Figure 8). More than 20 μg of unlabeled LUVs (150-nm radius) was required to dissociate 50% of the Va-LC bound to 1 μg of SUVs at 40 °C. Substantially more unlabeled LUVs were required at 10 °C. The latter was predicted from the temperature dependence of dissociation rates shown in Figure 7. At both temperatures, 1 μg of unlabeled SUVs was adequate to dissociate half of the bound Va-LC. This indicated that the dissociation constant for Va-LC bound to SUVs was 20 to several hundredfold lower than that for LUVs.

DISCUSSION

The properties of Va-LC interaction with membrane vesicles may provide two types of information in addition to determination of properties of this particular protein–membrane interaction. First of all, this reaction appeared to occur at the collisional limit and served as an illustration of how such situations are affected by particle size and number of binding sites per particle. Second, the properties of the interaction indicating very different intrinsic binding to SUVs vs LUVs may reflect basic thermodynamic differences between SUV and LUV structures. We will consider the association rate parameters first.

For a reaction where the number of binding sites is proportional to membrane surface area, the slope of a plot of k_{app} vs $1/R_v$ (Figure 3) provides information regarding reaction properties and can help to establish whether the reaction is collisionally limited. For a reaction that is entirely limited by collision, this plot will give a positive slope which passes through zero and from which the area per binding site can be estimated. Reactions that are far below the collisional limit will give a slope of zero. The value of k_{app} at this horizontal limit will be characteristic of a single receptor regardless of the size of the particle to which it is attached. An important property for membranes with a constant receptor density per unit of membrane area is that this plot must pass through zero; reactions that are not collisionally limited with small membrane particles will become collisionally limited for large particles (see Figure 3B). This follows from the fact that the number of recollisions occurring in the duration of an encounter complex is approximately proportional to R (Berg & Purcell, 1977) so that the number of recollisions will approach infinity as $1/R_v$ approaches zero.

For an example of how this property might be observed, Wei et al. (1982) estimated that prothrombin binding to SUVs (15-nm radius) was about 15% of the collisional limit. This association rate constant may be near the horizontal limit of the k_{app} vs $1/R$ plot (see Figure 3B). If the intrinsic association rate constant (k_+, eq 5) and surface area per binding site remain unchanged for larger particles, this reaction should begin to reach collisional efficiency (>50%) when the number of recollisions during an encounter complex is about 7 times that for small vesicles. This will theoretically occur for vesicles of ≥105-nm radius. Similarly, Silversmith and Nelsestuen (1986) observed that binding of the C5b-7 protein complex of complement to SUVs or LUVs was below the collisional limit. However, if the intrinsic association rate constant (k_+, eq 5) remains unchanged for cell membranes, this interaction may be collisionally limited for whole cells which are larger.

Another protein–membrane interaction type consists of discrete, widely separated protein receptors (or enzymes) on a membrane surface. For example, the kinetic properties for the prothrombinase complex assembled with one enzyme per vesicle have given k_{cat}/K_m ratios of 2×10^8 (Pusey & Nelsestuen, 1983) to 2×10^9 M^{-1} s^{-1} (van Rijn et al., 1984). Since this value is well below the collisional rate constant for prothrombin interaction with vesicles ($k_{coll} \sim 2 \times 10^{10}$ M^{-1} s^{-1}), it should represent the horizontal limiting value for k_{app} on the plot vs $1/R$. However, it is quite possible that this reaction will be collisionally limited for the biological reaction where multiple enzymes are present on a cell surface. For example, the collisional rate constant for prothrombin and a particle of 1-μm radius should be about 10^{12} M^{-1} s^{-1}. An association rate constant of 2×10^8 M^{-1} s^{-1} per enzyme would approach the collisional limitation for 5000 enzymes per particle (Nk_{app}). This number of enzymes appears to be quite reasonable for a single platelet (Rosing et al., 1985; Tracy et al., 1979). Dahlback and Stenflo (1980) found kinetics for the prothrombinase reaction on platelets that were similar to those found on vesicles. However, their kinetic studies were conducted below aggregation levels of platelets and at only about 300 enzymes per platelet. Surface saturation and formation of aggregates would increase N and ultimately should result in a situation where the apparent K_m for the reaction would increase due to the fact that k_{app}, the association constant for substrate–enzyme assembly (normally represented as k_1 of an enzyme reaction), will be in the collisionally limited region and will decrease with further increases in particle size (Figure 3B). Thus, K_m values obtained in studies with vesicles or isolated systems may be much lower than those which may typify the physiological circumstance.

The theoretical descriptions presented here utilize spherical particles while biological membrane particles may contain surface irregularities and different shapes. While a precise theoretical solution for other shapes would be difficult, it is important to note that the general behavior shown in Figure 3 results from a relationship between numbers of receptors and overall particle size. This general behavior will apply to particles of any shape. Furthermore, this type of kinetic behavior may be observed in modified form. For example, dense clusters of sites on a membrane would produce areas which function at the collisional limit, and kinetic properties would

be sensitive to the number of sites and the size of the cluster. Since protein collision with unpopulated areas of the membrane might not produce a binding event, k_{app} could be far below k_{coll}/N. Such clustering or dispersion of sites on a cell could even constitute methods for regulation of reaction kinetics.

For other protein–cellular binding interactions, the association rates can be as low as 10^4–10^5 M^{-1} s^{-1} (Kulczycki & Metzger, 1974; Anderson & Abraham, 1980). However, the receptor number per cell can reach 10^5, and the effective association rate constant may still approach the collisional limit (eq 2). Curved first-order dissociation rate plots are also a consistent feature of protein–cellular receptor binding studies (Belleman & Schade, 1983; Anderson & Abraham, 1980). As pointed out by Delisi and Wiegel (1981), curved dissociation plots are characteristic of reactions at the collisional limit as illustrated here in Figure 6 (see also eq 4). Since association and dissociation events are altered to the same extent, equilibrium binding constants of collisionally limited reactions should not vary with particle size.

Another interesting property of ligand–receptor interaction that correlates with collisional limitation is a difference in k_{dissn} measured by different methods; ligand that is bound to cells generally dissociates slower when measured by dilution methods than when measured by displacement by added ligand (Belleman & Schade, 1983; Anderson & Abraham, 1980). The dilution experiment allows the dissociated ligand to rebind to vacant receptors before it escapes (by diffusion) into the bulk solution whereas the displacement experiment blocks all receptors and prevents reassociation events. An interesting case of this behavior was reported by Esmon and Owen (1981), who observed that dissociation of thrombin from receptors in the profused heart was at least 10-fold slower than displacement by a competing ligand. Jakubowski et al. (1986) used the same receptor–ligand system and found that dissociation in the dilution experiment was essentially instantaneous ($t_{0.5} \ll 8$ min) for solubilized receptors but was more than an order of magnitude slower ($t_{0.5} \gg 60$ min) for cell-associated receptors. While several explanations for this behavior may be possible, these properties correlate with the expectation for a collisionally limited reaction. In general, kinetic properties can be very different for isolated, reconstituted receptors vs the same receptors on a cell surface.

There are many further considerations needed for accurate extrapolation of any to the biological situation. For example, the simple relationship between the probability of recollisions vs particle size must be corrected for various factors including mechanical agitation of the medium (Williams & Kutchai, 1986). In addition, the biological fluid may require consideration of extraordinary diffusion properties (Fulmer et al., 1981). Nevertheless, even within these limitations, it remains possible that many of these reactions could function at the collisional limit under biological conditions. In fact, the plasma concentrations of substrate together with the rate constant (or k_{cat}/K_m relationship) of a single complex may be naturally selected to function at the collisional limit under biological conditions. There would be no selective value to exceed the individual association rate constant (horizontal limit to k_{app} when plotted as in Figure 3) necessary to produce a collisionally limited reaction under the biological conditions where the enzyme or receptor functions.

Diffusional theory predicts that an interaction operating near the collisional limit and with a constant density of receptors per unit surface area will show slower dissociation from large vesicles than from small ones due to reassociation events. However, the dissociation rate of Va-LC was slower for SUVs than LUVs under all conditions (Figure 7). This property suggested a difference in the intrinsic affinity of Va-LC for the two types of membrane since the intrinsic equilibrium constant (K_I, eq 5) for a collisionally limited reaction is reflected in the dissociation rate constant (Delisi & Wiegel, 1981). Consequently, for Va-LC, the dissociation processes could not definitely demonstrate a collisionally limited process. However, curvature of the first-order dissociation plots was at least consistent with a collisionally limited process for each type of vesicle. However, the dissociation plots obtained were more curved than would be predicted by this property alone (Figure 6). Other explanations for curvature of dissociation rates are also possible (Dwyer & Bloomfield, 1981) and could result from negatively cooperative protein–protein or protein–phospholipid interactions. These factors will be evidenced in variations in K_I (eq 5) at different levels of membrane saturation.

Table II: Relationship of Type of Interaction to Thermodynamic Parameters[a]

type of interaction	ΔH	ΔS
hydrophobic	positive	positive
van der Waals	negative	negative
ionic	~0	positive
hydrogen bonding	negative	negative

[a] From Ross and Subramanian (1981).

The combined effects of slower association rates and faster dissociation rates contributed to at least a 20-fold decrease in the affinity of Va-LC for LUVs relative to SUVs. This selectivity for SUVs may provide the major explanation for the large variation in binding constants previously reported for Va-LC binding to vesicles (Pusey & Nelsestuen, 1984; van de Waart et al., 1983). However, in this study, the results indicated that the binding affinity for all vesicles tested remained in the nanomolar range or lower.

A basic thermodynamic difference in the binding of Va-LC to SUVs and LUVs was apparent from temperature studies. The difference in activation energies for the association and dissociation processes gave an approximation of ΔH for the reactions at equilibrium ($\Delta H_{SUV} = -16$ kcal/mol, $\Delta H_{LUV} \approx 0$ kcal/mol). Within the limitations of these estimates, it seemed clear that much of the free energy of binding to SUVs was the result of enthalpy changes (the ΔG for a reaction with a K_d of 10^{-11} M is about −16 kcal/mol) while binding to LUVs below 35 °C was almost exclusively entropic.

Anticipated contributions of entropy and enthalpy for different types of interaction have suggested that reactions with little or no enthalpy component and a large positive entropy are characteristic of ionic interactions (Table II). In this case, Va-LC–membrane binding would displace counterions and water molecules from the negatively charged phospholipid surface which would more than compensate for the loss of motion of the protein. Such interactions have also been used to explain the lack of K_{eq} variation with temperature for pentalysine–DNA binding to DNA (Lohman et al., 1980) and the increase in rate of various biochemical assembly processes (Lauffer, 1983). Only one other type of protein–membrane interaction has been found to show this behavior (Resnick & Nelsestuen, 1980).

The large negative ΔH and small ΔS observed with SUVs and with LUVs at high temperatures were not consistent with any single type of interaction (Table II) so that hydrophobic, van der Waals forces or hydrogen bonding may also contribute to these interactions. However, it seems unlikely that the actual type of protein–membrane contact would be very different for SUV vs LUV structures. The differences could

result from intramembrane events that contribute to the overall thermodynamic behavior. The highly curved outer monolayer of SUVs is known to impart several structural differences from large vesicles. For example, the area per phospholipid is about 40% larger in SUVs (Huang & Mason, 1978; Blume, 1979) which induces 2 atm of lateral pressure and effectively eliminates osmotically induced surface area increases (Sheetz & Chan, 1972; Sun et al., 1986). The latter can be 5–10% for LUVs (Li et al., 1986). Reduction in surface area is also resisted in SUVs as seen by a lower phase transition temperature and a smaller volume decrease upon transition to the gel state (Sheetz & Chan, 1972).

Suurkuusk et al. (1977) reported that SUVs are unstable and slowly fuse in the gel state to form LUVs. The enthalpy change for this reaction estimated from the excess enthalpies of the two phase transitions was about 2 kcal/mol of phospholipid. Two extreme cases can be considered. If the binding of Va-LC to SUVs reduced the surface strain, 2 kcal/mol of phospholipid will be the upper limit of the enthalpy difference between binding to SUVs vs LUVs. If Va-LC caused complete release of the enthalpy of SUV surface strain, interaction with eight phospholipids would provide the enthalpy of Va-LC binding observed here. Alternatively, if Va-LC bound to 60 phospholipids (the approximate number of phospholipids covered per protein when 75 proteins are present on a vesicle of 15-nm radius), it could partially reduce the enthalpy of each phospholipid by about 0.3 kcal/mol.

Another observation suggesting different interactions of Va-LC with SUVs vs LUVs was the effect of calcium ion on the dissociation rate. Calcium had a smaller effect on Va-LC dissociation from SUVs relative to LUVs. Increasing the calcium concentration from 0 to 3 mM (0.15 M total ionic strength) shortened the half-life of dissociation from LUVs by 7-fold but altered the dissociation from SUVs by only 2-fold (unpublished data). Furthermore, the difference became even greater at higher calcium concentrations. Such nonlinear dependence on calcium concentration may reflect a positive cooperativity expected when several counterions displace a single protein (Record et al., 1978).

Overall, this study provided some indication of the properties of interaction of Va-LC with membrane vesicles and also explored some properties of a collisionally controlled reaction. This study further illustrates the importance of examining rate as well as overall equilibrium binding properties. Extrapolation from vesicles to whole cells or to the biological system definitely requires consideration of collisional parameters. These general properties and their potential implications to many steps of the blood coagulation reactions as well as to other membrane systems are apparent.

Registry No. Factor Va, 65522-14-7.

REFERENCES

Anderson, C. L., & Abraham, G. N. (1980) *J. Immunol. 125*, 2734–2741.

Belleman, P., & Schade, A. (1983) in *Cell Surface Receptors* (Strange, P. G., Ed.) pp 101–109, Wiley, New York.

Berg, H. C., & Purcell, E. M. (1977) *Biophys. J. 20*, 193–219.

Berg, O. (1985) *Biophys. J. 47*, 1–14.

Berg, O. G., Winter, R. B., & von Hippel, P. H. (1981) *Biochemistry 20*, 6929–6948.

Bloomfield, V. A., & Lim, T. K. (1978) *Methods Enzymol. 48*, 415–494.

Blume, A. (1979) *Biochim. Biophys. Acta 557*, 32–44.

Boggs, J. M., & Moscarello, M. A. (1978) *Biochim. Biophys. Acta 515*, 1–21.

Cantor, C. R., & Schimmel, P. R. (1980) in *Biophysical Chemistry Part II*, p 628, W. H. Freeman, San Francisco, CA.

Chung, L., Kaloyanides, G., McDaniel, R., Mclaughlin, A., & Mclaughlin, S. (1985) *Biochemistry 24*, 442–452.

Cuatrecasas, P. (1971) *Proc. Natl. Acad. Sci. U.S.A. 68*, 1264–1268.

Dahlback, B., & Stenflo, J. (1980) *Eur. J. Biochem. 104*, 549–557.

Deamer, D., & Bangham, A. D. (1976) *Biochim. Biophys. Acta 443*, 629–634.

Delisi, C. (1983) *Methods Enzymol. 93*, 95–109.

Delisi, C., & Wiegel, F. W. (1981) *Proc. Natl. Acad. Sci. U.S.A. 78*, 5569–5572.

Dwyer, J. D., & Bloomfield, V. A. (1981) *Biopolymers 20*, 2323–2336.

Esmon, C. T. (1979) *J. Biol. Chem. 254*, 964–973.

Esmon, C. T., & Owen, W. G. (1981) *Proc. Natl. Acad. Sci. U.S.A. 78*, 2249–2252.

Frazier, W. A., Boyd, L. F., & Bradshaw, R. A. (1974) *J. Biol. Chem. 249*, 5513–5519.

Fulmer, A. W., Benbasat, J. A., & Bloomfield, V. A. (1981) *Biopolymers 20*, 1147–1159.

Gaber, B. P., & Peticolas, W. L. (1977) *Biochim. Biophys. Acta 465*, 260–274.

Gorrisen, H., Marsh, D., Rietveld, A., & de Kruijff, B. (1986) *Biochemistry 25*, 2904–2910.

Greenhut, S. F., Bourgeois, V. R., & Roseman, M. A. (1986) *J. Biol. Chem. 261*, 3670–3675.

Gruen, W. R., Marcelja, S., & Parsegian, V. A. (1984) *Recept. Ligands Intercell. Commun. 3*, 59–91.

Higgins, D. L., & Mann, K. G. (1983) *J. Biol. Chem. 258*, 6503–6508.

Hope, M. J., Bally, M. B., Webb, G., & Cullis, P. R. (1985) *Biochim. Biophys. Acta 812*, 55–65.

Huang, C., & Mason, J. T. (1978) *Proc. Natl. Acad. Sci. U.S.A. 75*, 308–310.

Illsley, N. P., Lin, H. Y., & Verkman, A. S. (1987) *Biochemistry 26*, 446–454.

Jackson, C. M., & Nemerson, Y. (1980) *Annu. Rev. Biochem. 49*, 765–811.

Jakubowski, H. L., Kline, M. D., & Owen, W. G. (1986) *J. Biol. Chem. 261*, 3876–3882.

Krieg, U. C., Isaacs, B. S., Yemul, S. S., Esmon, C. T., Bayley, H., & Johnson, A. E. (1987) *Biochemistry 26*, 103–109.

Kulczycki, A., Jr., & Metzger, H. (1974) *J. Exp. Med. 140*, 1676–1695.

Laemmli, C. K. (1970) *Nature (London) 227*, 680–685.

Lauffer, M. A. (1983) *Comments Mol. Cell. Biophys. 2*, 99–109.

Li, W., Aurora, T. S., Haines, T. H., & Cummins, H. Z. (1986) *Biochemistry 25*, 8220–8229.

Lindhout, T., Grovers-Riemslag, J. W. P., van de Waart, P., Hemker, H. C., & Rosing, J. (1982) *Biochemistry 21*, 5494–5502.

Livingstone, C. J., & Schachter, D. (1980) *J. Biol. Chem. 255*, 10902–10908.

Lohman, T. M., deHaseth, P. L., & Record, M. T., Jr. (1980) *Biochemistry 19*, 3522–3530.

Melchior, D. L., & Morowitz, H. J. (1972) *Biochemistry 11*, 4558–4562.

Mayer, L. D. (1983) Ph.D. Thesis, The University of Minnesota.

Mayer, L. D., Pusey, M. L., Griep, M. A., & Nelsestuen, G. L. (1983) *Biochemistry 22*, 6226–6232.

Mayer, L. D., Hope, M. J., & Cullis, P. R. (1986) *Biochim. Biophys. Acta 858*, 161–168.
Mclaughlin, S. (1977) *Curr. Top. Membr. Transp. 9*, 71–144.
Nelsestuen, G. L., & Lim, T. K. (1977) *Biochemistry 16*, 4164–4171.
Nesheim, M. E., Kettner, C., Shaw, E., & Mann, K. G. (1981) *J. Biol. Chem. 256*, 6537–6540.
Pusey, M. L., & Nelsestuen, G. L. (1983) *Biochem. Biophys. Res. Commun. 114*, 526–532.
Pusey, M. L., & Nelsestuen, G. L. (1984) *Biochemistry 23*, 6202–6210.
Pusey, M. L., Mayer, L. D., Wei, G. J., Bloomfield, V. A., & Nelsestuen, G. L. (1982) *Biochemistry 21*, 5262–5268.
Record, M. T., Jr., Anderson, C. F., & Lohman, T. M. (1978) *Q. Rev. Biophys. 11*, 103–178.
Resnick, R. M., & Nelsestuen, G. L. (1980) *Biochemistry 19*, 3028–3033.
Rosing, J., van Rijn, J. L. M. L., Bevers, E. M., van Dieijen, G., Comfurius, P., & Zwaal, R. F. A. (1985) *Blood 65*, 319–332.
Ross, P. D., & Subramanian, S. (1981) *Biochemistry 20*, 3096–3102.
Sackmann, E. (1984) in *Biological Membranes* (Chapman, D., Ed.) Vol. 5, p 132, Academic Press, New York.
Sheetz, M. P., & Chan, S. I. (1972) *Biochemistry 11*, 4573–4581.
Silversmith, R. E., & Nelsestuen, G. L. (1986) *Biochemistry 25*, 7717–7725.
Smoluchowski, M. (1917) *Z. Phys. Chem. 92*, 129–168.
Sun, S. T., Milon, A., Tanaka, T., Ourissen, G., & Nakatani, Y. (1986) *Biochim. Biophys. Acta 860*, 525–530.
Suurkuusk, J., Lentz, B. R., Barenholz, Y., Biltonen, R. L., & Thompson, T. E. (1976) *Biochemistry 15*, 1393–1401.
Tracy, P. B., Peterson, J. M., Nesheim, M. E., McDuffie, F. C., & Mann, K. G. (1979) *J. Biol. Chem. 254*, 10354–10361.
Tracy, P. B., Nesheim, M. E., & Mann, K. G. (1981) *J. Biol. Chem. 256*, 743–751.
van de Waart, P. (1984) Ph.D. Thesis, Rijkouniversiteit Limburg, Maastricht, The Netherlands.
van de Waart, P., Bruls, H., Hemker, H. C., & Lindhout, T. (1983) *Biochemistry 22*, 2427–2432.
van de Waart, P., Hemker, H. C., & Lindhout, T. (1984) *Biochemistry 23*, 2838–2842.
van de Waart, P., Visser, A. J. W., Hemker, H. C., & Lindhout, T. (1987) *Eur. J. Biochem. 164*, 337–343.
van Rijn, J. L. M. L., Grovers-Riemslag, J. W. P., Zwaal, R. F. A., & Rosing, J. (1984) *Biochemistry 23*, 4557–4564.
Wei, G. J., Bloomfield, V. A., Resnick, R. M., & Nelsestuen, G. L. (1982) *Biochemistry 21*, 1949–1959.
Wiegel, F. W. (1984) *Recept. Ligands Intercell. Commun. 3*, 3–21.
Williams, J. B., & Kutchai, H. (1986) *Biophys. J. 49*, 453–458.
Worman, H. J., Brasitus, T. A., Dudeja, P. K., Fozzard, H. A., & Field, M. (1986) *Biochemistry 25*, 1549–1555.